RNA ligands activate the Machupo virus polymerase and guide promoter usage

Jesse D. Pyle[a,b] and Sean P. J. Whelan[a,b,1]

[a]Department of Microbiology, Harvard Medical School, Boston, MA 02115; and [b]PhD Program in Virology, Harvard Medical School, Boston, MA 02115

Edited by Jeffrey S. Kieft, University of Colorado Anschutz Medical Campus, Aurora, CO, and accepted by Editorial Board Member Michael F. Summers April 12, 2019 (received for review January 16, 2019)

Segmented negative-sense (SNS) RNA viruses initiate infection by delivering into cells a suite of genomic RNA segments, each sheathed by the viral nucleocapsid protein and bound by the RNA-dependent RNA-polymerase (RdRP). For the orthomyxovirus influenza and the bunyavirus La Crosse, the 5′ end of the genomic RNA binds as a hook-like structure proximal to the active site of the RdRP. Using an in vitro assay for the RNA-dependent RNA-polymerase (RdRP) of the arenavirus Machupo (MACV), we demonstrate that the 5′ genomic and antigenomic RNAs of both small and large genome segments stimulate activity in a promoter-specific manner. Functional probing of the activating RNAs identifies intramolecular base-pairing between positions +1 and +7 and a pseudotemplated 5′ terminal guanine residue as key for activation. Binding of structured 5′ RNAs is a conserved feature of all SNS RNA virus polymerases, implying that promoter-specific RdRP activation extends beyond the arenaviruses. The 5′ RNAs and the RNA binding pocket itself represent targets for therapeutic intervention.

RNA-dependent RNA polymerase | RNA replication | arenavirus | segmented negative-sense RNA virus | influenza virus

The large (L) protein of arenaviruses, a family of viruses that include Lassa, lymphocytic choriomeningitis (LCMV), and Machupo (MACV), is the RNA-dependent RNA-polymerase (RdRP) and the cap-dependent endonuclease that liberate host cell mRNA-capped primers for mRNA synthesis. The viral genome comprises two ribonucleoprotein (RNP) segments, each encoding two genes. The small (S) segment encodes the nucleocapsid protein (NP) that encases the genomic and antigenomic RNAs, as well as the attachment and membrane fusion glycoprotein complex (GPC). The large (L) segment encodes the L protein and a small matrix protein (Z) involved in particle assembly. The ambisense arrangement of the two genes on each segment necessitates transcription of both the genomic and antigenomic RNPs by L protein (Fig. 1*A*).

During mRNA synthesis, the cap-dependent endonuclease of L cleaves host cell cytoplasmic mRNAs to yield short capped primers for the RdRP (1–7). Transcription of the genomic S and L segments results in the synthesis of the NP and L mRNAs, respectively, translation of which is requisite for viral genome replication (8–10). During replication, the RdRP initiates at position +2 on the promoter to generate a cytidylyl(5′-3′)guanosine 5′-triphosphate (pppGpC) dinucleotide primer that realigns, facilitating base pairing between the C and a G at position +1 of the template. Subsequent elongation by the RdRP, coupled with encapsidation of the nascent RNA by NP, results in the synthesis of antigenomic RNPs with a pseudotemplated pppG residue at the 5′ terminus (1, 2, 11–14). The antigenomic RNPs are also used as templates for viral mRNA synthesis, producing the GPC and Z mRNAs from the S and L segments, respectively. The antigenomic RNPs also serve as template for pppGpC primed replication to produce more genomic RNPs.

All segmented negative-sense (SNS) RNA viruses encode an RdRP and cap-dependent endonuclease. For the trisegmented bunyavirales, as exemplified by La Crosse (LACV), those activities reside within an L protein analogous to that of arenaviruses. In the case of influenza A virus, an eight segment-containing orthomyxovirus, a heterotrimer of three viral proteins PA, PB1, and PB2, forms the functional equivalent of the arena/bunya L (Fig. 1*B*). The PA subunit contains the cap-dependent endonuclease activity that cleaves pre-mRNA cap structures in the nucleus to prime mRNA synthesis. Atomic structures of the influenza polymerase (15–18), and a partial structure of LACV L (19), reveal U-shaped arrangements with endonuclease and cap-binding domains flanking a core RdRP (Fig. 1 *C*, *Left* and *Middle*). For influenza, the core is formed by PA-C and PB1 (RdRP) subunits, with solvent-exposed PB2 (cap-binding) and PA (endonuclease) domains positioned on either side of a product exit channel (15–17). There are no atomic-level structures of arenavirus L proteins, but negative-stain electron microscopy of MACV L supports a similar domain arrangement (20) (Fig. 1 *C*, *Right*).

Binding of the 5′ end of the viral RNA orders the catalytic residues of the influenza and LACV RdRP. For influenza, the 5′ 10 nucleotides of the virion RNA (vRNA) fill a groove between the PA-C and PB1 subunits (Fig. 1 *C*, *Middle*) (16). An analogous pocket between the N-terminal and core RdRP domains of LACV L binds a similar 5′ vRNA (Fig. 1 *B* and *C*). Assays of influenza virus polymerase function in vitro demonstrate that intramolecular base pairing within the 5′ terminus is required for polymerase binding and RNA synthesis (21–28). A lack of in vitro assays for the RdRP activity of LACV or any member of the *Bunyavirales* precludes a mechanistic examination of the role of RNA binding.

Significance

Atomic structures of the polymerase–endonuclease complex of the orthomyxovirus influenza and the orthobunyavirus La Crosse—two distinct segmented negative-sense (SNS) RNA viruses—demonstrate that binding of the genomic 5′ RNA rearranges the catalytic residues of the RNA-dependent RNA-polymerase (RdRP). Working with the arenavirus, Machupo, we demonstrate that 5′ RNAs from the genomic and antigenomic copies of both segments activate the RdRP in conjunction with a specific promoter. This study builds upon structural studies with two different SNS RNA viruses to reveal a previously unappreciated mechanism of RNA-guided promoter-specific polymerase regulation in SNS RNA viruses. The conservation of activating RNA elements among the polymerase–endonuclease complexes of SNS RNA viruses suggests new avenues for developing antiviral therapeutics.

Author contributions: J.D.P. and S.P.J.W. designed research; J.D.P. performed research; J.D.P. and S.P.J.W. analyzed data; and J.D.P. and S.P.J.W. wrote the paper.

The authors declare no conflict of interest.

This article is a PNAS Direct Submission. J.S.K. is a guest editor invited by the Editorial Board.

[1]To whom correspondence should be addressed. Email: sean_whelan@hms.harvard.edu.

This article contains supporting information online at www.pnas.org/lookup/suppl/doi:10.1073/pnas.1900790116/-/DCSupplemental.

Published online May 9, 2019.

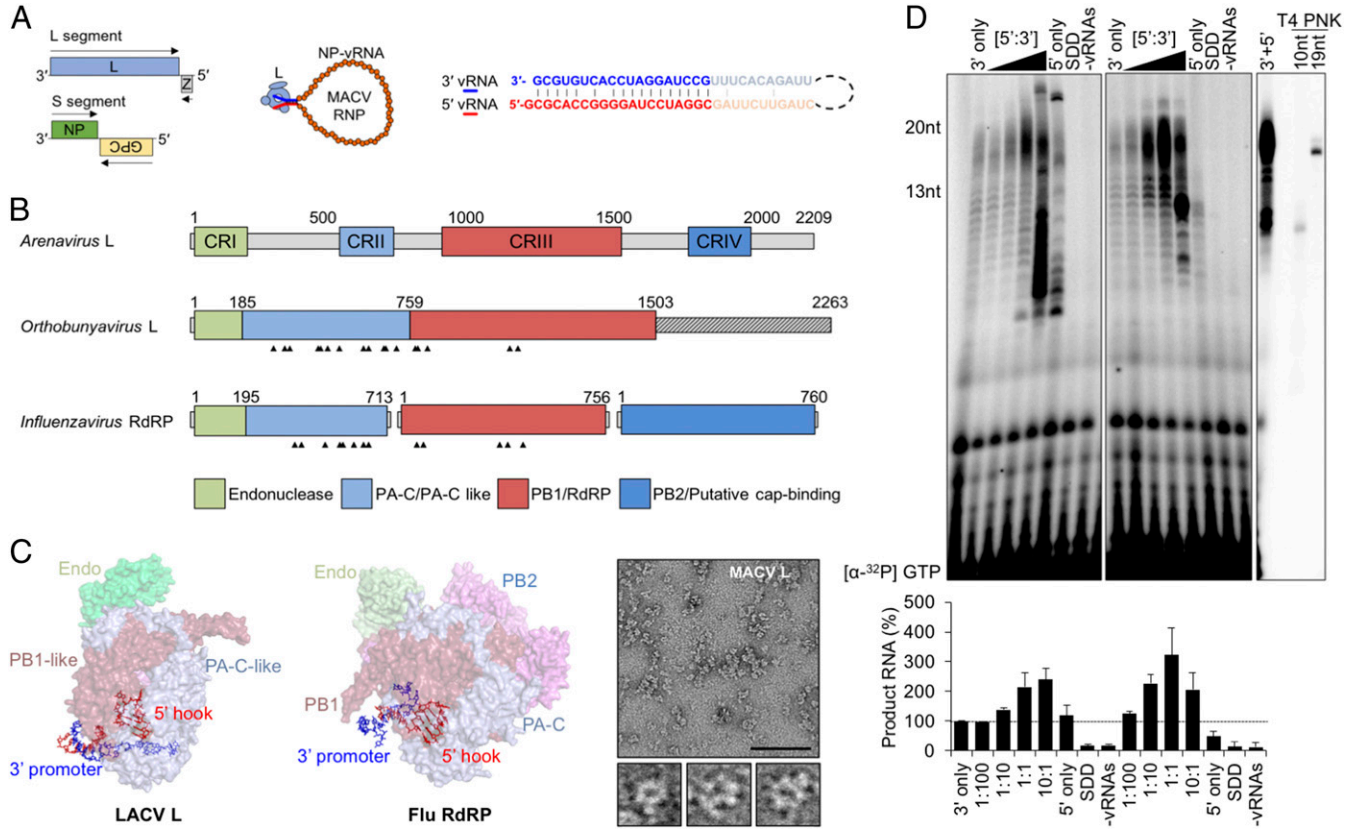

Fig. 1. The 5′ genomic termini regulate the functions of SNS RNA polymerases. (*A*) The bisegmented ambisense arenavirus genome and the viral ribonucleoprotein (RNP), showing NP-encapsidated vRNA (orange) bound by L (light blue) with pseudocomplementary termini (bolded blue and red text, respectively). Viral ORFs are shown as colored boxes in the genome, and the arrows indicate coding sense. (*B*) Domain organization of the SNS RdRP. Four conserved regions (CRI to IV) of the arenavirus L protein are illustrated in colored boxes. The *Orthobunyavirus* and *Influenzavirus* domain labels are based on available crystal structures. The 5′ vRNA-interacting residues are indicated with arrowheads. (*C*) Positions of the 5′ vRNA hook-like structures in LACV L (*Left*, PDB ID code 5AMQ) and influenza A polymerase (*Middle*, Flu RdRP, PDB ID code 4WSB). The domains are colored according to the illustration in *A*. (*C*, *Right*) Visualization of purified MACV L by negative-stain electron microscopy. Three particles resembling the previously described L architecture (20) are shown below the larger micrograph image. (Scale bar: 100 nm.) (*D*) Stimulation of in vitro RNA synthesis by the 5′ vRNA. (*D*, *Left*) Increasing amounts of the 20-nt 5′ vRNA ligand were added to reactions relative to the 3′ template ([5′:3′]). Reactions with catalytically inactive L (SDD) or no added vRNA (–vRNAs) are shown. (*D*, *Middle*) Parallel reactions performed using a minimal activating ligand for RNA synthesis. (*D*, *Right*) A reaction performed in the presence of the 13-nt 5′ vRNA, alongside oligoribonucleotide primers end labeled by T4 polynucleotide kinase (PNK). Products of RNA synthesis were separated on denaturing 20% polyacrylamide-urea gels, visualized, and quantified as described in *Materials and Methods*, and % RNA synthesis is depicted in bar graphs. Error bars represent the SD from the mean of three independent experiments.

The conservation of 5′ RNA binding to the polymerase of influenza and LACV led us to examine how 5′ RNA binding influences the RdRP of arenaviruses. Using an in vitro RdRP assay for MACV, we demonstrate that binding of the 5′ vRNA and the 5′ RNA from the complementary antigenomic strand (cRNA) stimulates the RdRP. Activation depends on intramolecular base-pairing events in the 5′ RNA and stimulates the activity of the polymerase on the corresponding 3′ vRNA or 3′ cRNA promoter. The pseudotemplated 5′ G residue is also required for activation, demonstrating that the activating RNA is a product of genome replication. Conservation of 5′ RNA binding among polymerases of all SNS RNA viruses suggests that similar promoter-specific regulation may extend beyond the arenaviruses.

Results

Stimulation of the RNA-Dependent RNA Polymerase of Machupo Virus by an RNA Ligand. Using MACV RdRP expressed and purified from insect cells (*SI Appendix*, Fig. S1), we examined whether the 5′ genomic RNA (5′ vRNA) impacts RNA synthesis in vitro. The prime-and-realign mechanism of initiation of arenavirus replication results in the addition of a nontemplated 5′ terminal residue termed G0. We used a 20-nt RNA comprising G0 and residues 1 to 19 of the 5′ vRNA, which are identical in sequence for the S and L segments (Fig. 1*A* and *SI Appendix*, Fig. S2*A*). In this assay, purified L is incubated with a synthetic RNA corresponding to the 19-nt 3′ vRNA S segment promoter (Fig. 1*A*) in the presence of nucleoside triphosphates supplemented with [α^{32}P]-GTP and the products detected by phosphoimage analysis following electrophoresis on a denaturing 20% polyacrylamide gel (Fig. 1*D*). Supplementing the reactions with increasing amounts of the 20-nt 5′ vRNA results in a 2.5-fold increase in the accumulation of the 20-nt product of prime-and-realign synthesis from the S segment 3′ vRNA promoter (Fig. 1 *D*, *Left*). Reactions that contain a 10-fold excess of this 5′ vRNA ligand, or that omit the 3′ template, result in the accumulation of aberrant products (Fig. 1 *D*, *Left*). Omission of the 3′ template RNA results in the accumulation of products that likely originate by 5′ pppGpC primed elongation from the 3′ CpG terminus of that RNA (Fig. 1 *D*, *Left*). As expected, reactions containing catalytically inactive RdRP, or in which the 5′ and 3′ RNA are omitted, fail to accumulate detectable products (Fig. 1 *D*, *Left*).

To identify a minimal element within the 5′ vRNA for activation of the RdRP, we tested a panel of truncated RNAs. As the activating RNA was progressively truncated from the 3′ end, we observed an increase in the accumulation of RNA products up to a maximal eightfold stimulation for a 13-nt RNA comprising residues G0 to U12 (5′ vRNA12) (*SI Appendix*, Fig. S2).

Truncation of the 5′ end of the RNA by 3 nt results in a loss of stimulatory activity, demonstrating the importance of the correct 5′ terminus (*SI Appendix*, Fig. S2*B*). The precise length of the stimulatory RNA, however, was not critical as ligands corresponding to 0 to 7 and 0 to 23 retained activating functions (*SI Appendix*, Fig. S2*B*). Differences in activation among the truncated RNAs likely reflect their ability to adopt specific RNA structures or serve as templates for pppGpC primed synthesis. To determine whether the products of RNA synthesis observed in the presence of the activating 5′ vRNA include significant polymerase extension from the 5′ vRNA, we used a 3′ dideoxy-C variant of the 13-nt 5′ vRNA (*SI Appendix*, Fig. S3). The dideoxy 3′ terminus of that 13-nt vRNA chemically precluded its use for extension yet stimulated RdRP activity to the same extent (*SI Appendix*, Fig. S3).

The Activating RNA Is Sequence-Specific. The 11-nt RNAs visible in the influenza and LACV polymerase structures share no obvious sequence similarity with the 5′ RNA of MACV (Fig. 2*A*). Consistent with activation requiring a specific RNA ligand, neither the influenza nor the LACV 5′ RNAs activated the MACV RdRP (Fig. 2*B*). Further support of this RNA specificity is provided by functional analysis of different MACV sequences. Full-length S segment sequences cluster in three groups: a conserved (CONS) 5′ sequence (29–31), sequences with perfect complementarity (COMP) to the 3′ promoter vRNA, and the S segment reference (REF) (GenBank accession no. NC_005078) (Fig. 2*A*). Testing each of those RNAs demonstrated that only the CONS 5′ RNA stimulates MACV L, underscoring that the ligand functions in a sequence-specific manner (Fig. 2*B*).

Activating RNA Stimulates Polymerase on Specific Promoters. The ambisense nature of gene expression in arenaviruses results in both genomes (vRNA) and antigenomes (cRNA) functioning as templates for mRNA synthesis. The two promoters are related in sequence, with only two differences over 19 nt (Fig. 2*A*, CONS and cRNA sequences). Testing each possible permutation of 5′ RNA and 3′ promoter demonstrated that the 5′ vRNA activates the RdRP on the 3′ vRNA but not the 3′ cRNA promoter (Fig. 2*C*). Correspondingly, the 5′ cRNA stimulated RdRP activity on the 3′ cRNA and not the 3′ vRNA promoter (Fig. 2*C*). This result demonstrates that the correct 5′ RNA is required to stimulate RdRP activity in a promoter-specific manner.

The S and L 5′ vRNA sequences are identical, but the 3′ vRNA promoters differ. Accordingly, the antigenomic S and L cRNAs contain identical 3′ promoters but distinct 5′ RNAs (*SI Appendix*, Fig. S4*A*). The S segment specificity elements are at positions +6 and +8 in both the vRNA and cRNA (Figs. 1*A* and 2*A*), and the L segment specificity element is at position +8 (32). MACV L effectively initiates on the S and L segment vRNA and cRNA promoters (*SI Appendix*, Fig. S4*B*) but is preferentially activated by the presence of template–ligand combinations, with mismatches at positions +6 and +8 (*SI Appendix*, Fig. S4*A*). Perfectly double-stranded panhandle termini, or those in which there is only one mismatch, show inhibited or near background (3′ promoter alone) levels of RNA synthesis (*SI Appendix*, Fig. S4 *A* and *B*). Moreover, activated L has greater activity on the S segment promoters compared with those of the L segment, with the highest levels of RNA synthesis attributed to the vRNA promoters of the S segment (*SI Appendix*, Fig. S4*C*). This analysis demonstrates that specific 5′ RNAs dictate optimal synthesis from the four viral promoters. The relative efficiency of the correct 5′ RNA promoter combinations results in a gradient of activities where S vRNA > S cRNA > L cRNA = L vRNA (*SI Appendix*, Fig. S4*C*).

Terminal Features of the MACV Activating RNA. The activating 5′ RNAs contain a terminal triphosphate G0 as a result of the prime-and-realign mechanism for replication. To determine whether the phosphorylation status of G0 alters the ability of the RNA to

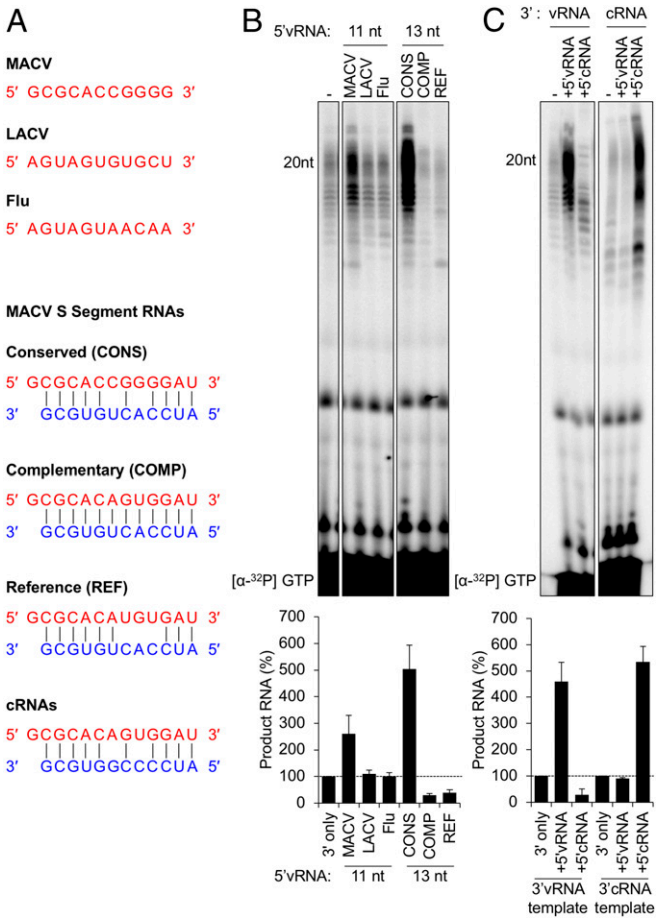

Fig. 2. Activation of MACV L by the 5′ ligand is sequence-specific. (*A*, *Upper*) Comparison of the MACV conserved terminal 5′ vRNA sequence with La Crosse virus (LACV) and influenza (Flu) RdRP atomic structures. (*A*, *Lower*) MACV 5′:3′ v/cRNA duplexes containing S segment sequences represented in GenBank. (*B*) MACV L is specifically activated by a conserved arenavirus sequence. In vitro RNA synthesis reactions were performed as in Fig. 1. The gel labels for the *Middle* and *Right* hand panels correspond to the oligo sequences shown in *A* and *B*, respectively. (*C*) The 5′ vRNA and 5′ cRNA of MACV mediate activation of L, in a template-dependent manner. In vitro RNA synthesis reactions were performed with either a 3′ vRNA template (*Left*) or a 3′ cRNA template (*Right*). For each template, a 12-nt 5′ vRNA or 5′ cRNA ligand was included. Products of RNA synthesis were visualized and quantified as in Fig. 1, and the relative changes in RNA accumulation are shown as bar graphs below the gel images in *B* and *C*. Error bars for all graphs represent the SD from the mean of three independent experiments.

stimulate polymerase activity, we tested hydroxyl-, monophosphate-, and triphosphate-modified 5′ vRNA ligands. All three terminal chemistries stimulated the RdRP (*SI Appendix*, Fig. S5), with the strongest activation occurring with a monophosphate 5′ vRNA12. Deletion of the nontemplated G0 disrupted the activation of MACV L in vitro (*SI Appendix*, Fig. S5), indicating that the functionality of the 5′ vRNA12 ligand depends upon the product of the prime-and-realign genome replication mechanism. Addition of 3A residues upstream of the G0 5′ terminus (AAA-5′) reduced activation by 50% (*SI Appendix*, Fig. S5). These results demonstrate that optimal activation is achieved when the RNA contains a 5′ terminal, nontemplated G0 residue.

RNA Binding Activates the Polymerase. We next examined whether sequential binding to the 5′ and 3′ vRNAs influences stimulation (Fig. 3*A*). Stimulation of RdRP activity does not depend upon sequential RNA binding as preincubation of L with one RNA

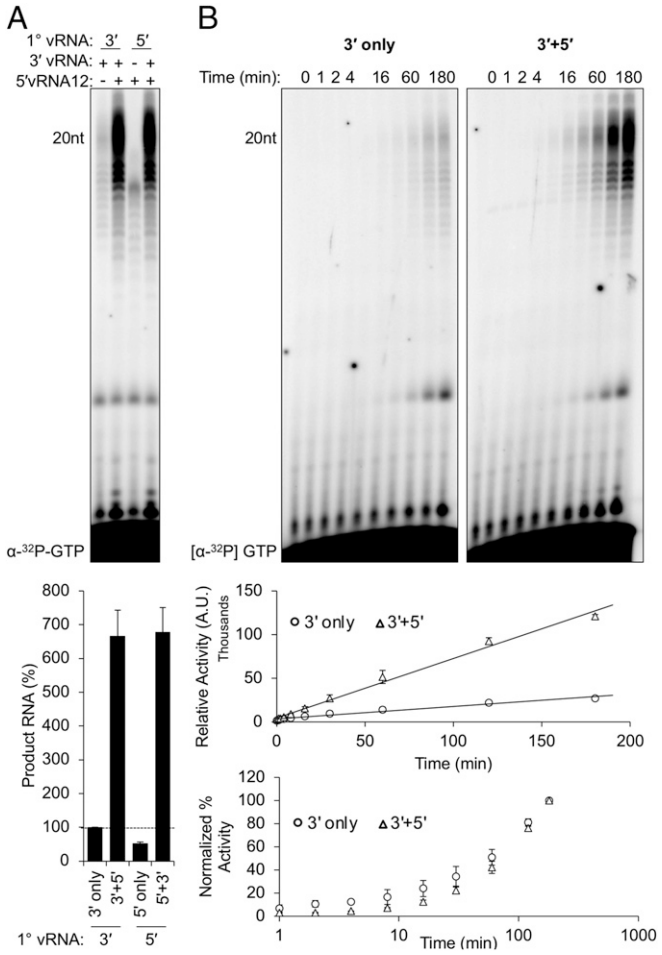

Fig. 3. The MACV 5′ hook ligand functions as a bona fide activator of RNA synthesis. (*A*) Activation of MACV L occurs independently of sequential 3′ or 5′ vRNA addition. Products of RNA synthesis were visualized and quantified as in Fig. 1, and the relative changes in RNA accumulation are shown in a bar graph below the gel image. (*B*) Temporal analyses of MACV L activity in the absence (*Left*, 3′ only) or presence (*Right*, 3′ + 5′) of the 5′ vRNA ligand. (Upper graph) Nonnormalized quantification of RNA product accumulation in the absence (circles) or presence (triangles) of the 5′ ligand. (Lower graph) The normalized percent activity of MACV L in the absence (circles) or presence (triangles) of the 5′ ligand. All in vitro RNA synthesis reactions were performed as in Figs. 2 and 3 with equimolar concentrations of 3′ promoter and 5′ ligand, except in A, where either the 5′ (lane 1) or 3′ (lane 3) vRNAs were omitted from the reactions.

followed by the addition of the second just before NTP supplementation resulted in the same activity irrespective of the order of addition (Fig. 3*A*). To determine whether the activating RNA alters the kinetics of RNA synthesis, we measured product accumulation over time. The 20-nt full-length RNA product was visible by 4 min post NTP addition in the presence of the activating RNA whereas similar product levels required 16 min of synthesis in unstimulated reactions (Fig. 3*B*). Over the course of a 3-h reaction, we observed an ∼4.8-fold increase in product accumulation in the presence of the 5′ ligand (Fig. 3*B*, upper graph). A comparison of the rate of increase revealed that the relative rates of RNA synthesis are equivalent, regardless of the presence or absence of the 5′ RNA (Fig. 3*B*, lower graph). We interpret this result as demonstrating that the 5′ vRNA12 ligand activates a pool of otherwise inactive or low-functioning MACV L, resulting in earlier product detection.

MACV L Activation Requires a Structured Element Within the 5′ vRNA. The 5′ RNAs bound to the LACV and influenza polymerase form a hook-like structure involving canonical and noncanonical intramolecular base-pairing events. The 5′ sequences of LACV and influenza share the 6-nt AU-rich terminal motif (5′-AGUAGU-3′, Fig. 2*A*) but adopt distinct structures with unique polymerase interactions. If structure within the MACV activating ligands is important for stimulation of polymerase activity, their GC-rich sequence would likely adopt a distinct structure. An mfold secondary structure prediction suggests a base-pairing interaction between C1 and G7, and G2 and C6 (Fig. 4*A*). Mapping the determinants within the 5′ vRNA12 ligand for polymerase activation revealed that substitutions at G0, C1, C6, G7, and G10 result in a complete loss of activation (Fig. 4*B*). The finding that C1, G7, and C6 substitutions impede polymerase

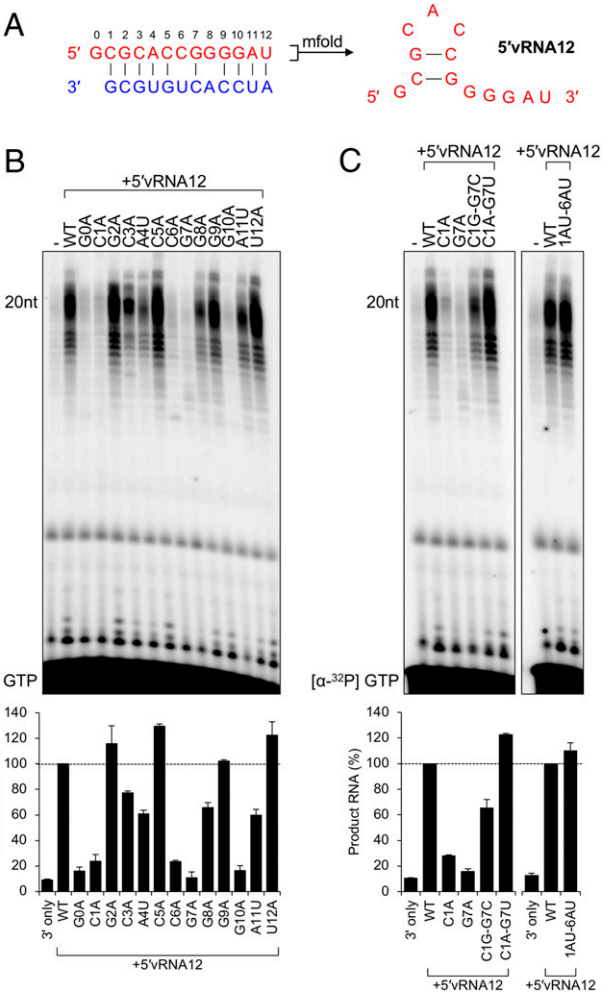

Fig. 4. Identification of essential residues for a functional activating 5′ vRNA12 ligand. (*A*) Predicted structure of the terminal 5′ vRNA ligand of MACV, determined by mfold as described in *Materials and Methods*. (*B*) Adenine/uracil mutagenesis of the MACV 12-nt 5′ vRNA ligand (5′vRNA12). In vitro RNA synthesis reactions were performed as in Fig. 2 with equimolar concentrations of 3′ promoter and 5′ ligand. Products of RNA synthesis were visualized and quantified as in Fig. 1, and the relative changes in RNA synthesis are shown in a bar graph below the gel image. (*C*) Substitution of predicted base-pairing events restores 5′ ligand functionality. The *Left* shows L-synthesized products for substitutions at the C1–G7 predicted base-pairing site. The *Right* shows the substitution of positions 1 to 2 and 6 to 7 with A-U to restore the predicted hook-like structure. All sequence names correspond to the mutant vRNAs described in *SI Appendix*, Table S2. Products of RNA synthesis were visualized and quantified as in Fig. 1, and the relative changes in RNA accumulation are shown in bar graphs below each gel image.

activation, whereas mutation of G2 is inert, is inconsistent with a requirement for canonical base pairing between G2 and C6. The loss of activation following mutation of position G0 is consistent with the finding that its deletion suppresses activation (*SI Appendix*, Fig. S5).

For influenza virus, in addition to the bases within the 5′ RNA participating in intramolecular base-pairing interactions, other residues are involved in direct interactions with the polymerase, and some residues base pair with the 3′ vRNA template (15). Whether similar interactions between the MACV 5′ vRNA12 and polymerase account for the loss of activity associated with C3, A4, and G10 substitutions is uncertain. The WT MACV 5′ vRNA12, however, stimulates RdRP activity on a C10A mutant promoter, which is inconsistent with a canonical base-pairing interaction between G10 of the activating ligand and C10 of the promoter (*SI Appendix*, Fig. S6).

The MACV 5′ cRNA12 ligand differs from the 5′ vRNA12 at positions +6 and +8 (Fig. 2*A*), corresponding to the sites that are mismatched within a 5′ and 3′ vRNA predicted panhandle structure (Fig. 1*A*). Mutagenesis of this 5′ cRNA12 ligand revealed a nearly identical pattern of critical residues for activating RNA synthesis on a 3′ cRNA template (*SI Appendix*, Fig. S7). The U8A mutation, one of the sites differing from the 5′ vRNA12 ligand, results in an increase in the abundance of prematurely terminated products. A comparison of results from mutational studies of the 5′ vRNA12 and 5′ cRNA12 ligands suggests that both adopt structures that require base pairing between positions C1 and G7 for activation of the MACV L protein on the corresponding promoter elements.

Activation Requires a Base-Pairing Interaction Between C1 and G7. To further test the functional importance of the predicted C1–G7 base pairing, we generated a panel of RNAs with restorative mutations (Fig. 4*C*). The mutagenesis data above (Fig. 4*B*) are incompatible with a canonical base-pairing event between positions 2 and 6, but we included those positions in this analysis in an attempt to determine whether they might be involved in noncanonical interactions. Base switching (G2C–C6G) or transition mutagenesis (G2A–C6U) resulted in polymerase activation of ∼40% and ∼60%, respectively (*SI Appendix*, Fig. S8). The same results were observed with transversion substitutions (G2U–C6A) and the G2U mutation alone (*SI Appendix*, Fig. S8). This result highlights the importance of C6 and underscores that the identity of the base at position +2 is not critical for activation.

Point mutations to the predicted C1–G7 interaction disrupt the activating function of the 5′ vRNA12 ligand (Fig. 4*B*). Restoring the predicted base-pairing event by swapping the bases (C1G–G7C) or through introducing transition mutations (C1A–G7U) partially (∼60%) or completely (∼120%) restored the activating function of the 5′ vRNA12 ligand (Fig. 4*C*). Similar activation was observed with the same restorative mutations in the 5′ cRNA12 ligand (*SI Appendix*, Fig. S7*C*). Activation of L was still apparent following the introduction of transversion mutations to positions +1 to +2 and +6 to +7 (1AU-6AU), demonstrating that activation is dependent upon the restored interaction between bases +1 and +7, and to some extent +2 and +6, independent of purine or pyrimidine placement within the stem of the hook-like structure (Fig. 4*C*). The results likely explain the stimulatory effects of the truncated 5′ vRNA containing residues 0 to 7 (*SI Appendix*, Fig. S2*B*). Taken together, these results provide evidence of a base-pairing interaction between positions 1 and 7 and demonstrate that the activation of MACV L requires a structure present at the 5′ terminus of the viral RNAs.

Discussion

The principal finding of our study is that viral RNA ligands activate the RdRP activity of Machupo virus L. Those RNA ligands are provided by the 5′ termini of the viral genomic or antigenomic RNA or short RNAs that correspond to them. The RNA ligands activate the polymerase in a promoter-specific manner such that the 5′ vRNA ligand activates polymerase for the 3′ vRNA and not 3′ cRNA promoter, and the 5′ cRNA ligand activates only on the 3′ cRNA promoter. The activating ligands require intramolecular base-pairing interactions, implying that they are structured elements similar to the 5′ hook-like RNAs that organize the active-site residues of the RdRP of influenza and LACV. Collectively, this work demonstrates that structured 5′ RNA ligands are a conserved activating element for all SNS virus polymerases and suggests that the structured RNA as well as its binding site within the polymerase are new targets for potential therapeutic intervention.

Promoter Specificity. For MACV, the activating vRNA and cRNA ligands are predicted to adopt similar structures and share extensive sequence similarity, yet activate the RdRP in a promoter-dependent manner. This RNA-guided promoter selectivity of the activated polymerase must involve the two variant positions (6, 8) within the respective 5′ RNAs and 3′ promoters (*SI Appendix*, Fig. S4). Our earlier work demonstrated that positions 2 to 5 of the 3′ promoter are required for L binding and that the 5′ and 3′ RNAs are bound as single-stranded ligands rather than a duplex structure (20). The mismatches in base pairing between the termini at positions 6 and 8 likely play a key role in the ability of the 5′ RNA to adopt a structure—leaving the key 3′ promoter residues accessible for L binding (Fig. 5*A*). The canonical base-pairing interaction involving positions C1–G7 of the activating RNAs, coupled with the mismatches at positions 6 and 8, likely favors the formation of a structure within the 5′ end, facilitating strand separation between the promoter and the 5′ RNA. Consistent with this, the ability of any given 5′ RNA to stimulate the polymerase correlates with mismatches at positions +6 and +8. Elimination of the mismatch at position 6—as seen for the L segment in both the vRNA and the cRNA—results in a reduction of RdRP activity. This implies that position 8 is a key determinant of the promoter selectivity of the activated RdRP. Structural analysis of the MACV L protein together with the activating RNAs will be required to fully understand the mechanism by which the RNA results in promoter-specific activation.

Functions of the 5′ RNA Structure in Segmented Negative-Strand RNA Viruses. The demonstration that the RdRP is an RNA-activated enzyme and that RNAs corresponding to the 5′ S and L vRNA and cRNA dictate distinct levels of activity in both a promoter- and segment-specific manner reveals a previously unappreciated aspect of the regulation of gene expression in arenaviruses. The absence of a distinct cap-primed transcription assay, however, precludes a determination of whether the activation is required for segment transcription, replication, or both. A confounding factor in resolving this question without an in vitro cap-primed transcription assay is that both vRNA and cRNA are templates for transcription and replication. In the *Bunyavirales*, where only one segment is ambisense, the lack of any in vitro polymerase assay precludes testing of whether the 5′ RNA activates transcription or replication. Extending from the structural studies of influenza and LACV, we favor the idea that the RNA activates a pool of polymerase, making it competent for initiation, and that, in the absence of the RNA, the active site of the polymerase can adopt the correct conformation less efficiently. This would imply that the activated polymerase is more competent for both transcription and replication. Sequencing of influenza virus-infected cells identified highly abundant short viral RNAs that correspond to the 5′ vRNA of each segment (33, 34). Suppression of specific svRNA levels correlated with a reduction in the corresponding vRNA levels, while having minimal effect on mRNA and cRNA accumulation (33, 34), perhaps suggesting that the 5′ RNA is required for replication but not cap-primed transcription. Binding of the 5′ cRNA ligand to the influenza polymerase

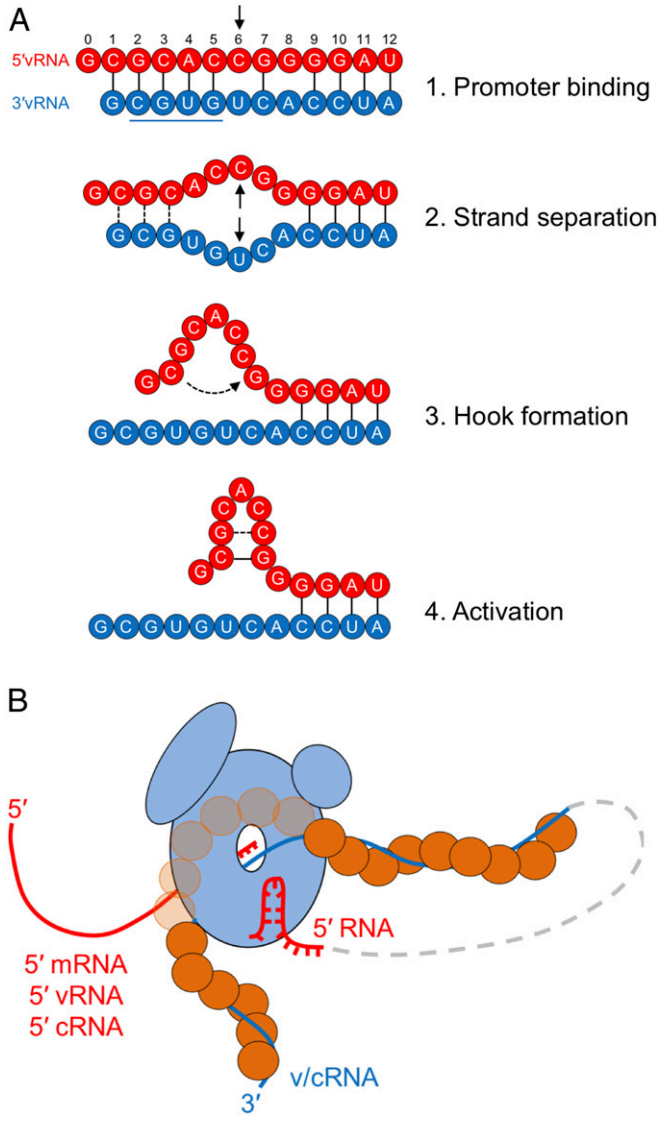

Fig. 5. Model of arenavirus L activation by a 5′ hook structure present in the terminal genomic (vRNA) and antigenomic (cRNA) RNA segments. (*A*) Proposed four-step mechanism of L initiation and activation by the 5′ vRNA ligand (red). The underlined 3′ vRNA sequence represents the previously identified motif for promoter recognition by MACV L (20). (*B*) A model of the activated arenavirus RNA synthesis complex. L (light blue) is shown bound to the 3′ v/cRNA (blue line), which is encapsidated by the viral nucleoprotein (orange circles). The nascent 5′ RNA (red line) is shown exiting to the left of L. The activating 5′ hook (red line) is also illustrated as being bound by L. The intermediate RNP is depicted as a dashed gray line connecting the 3′ RNA and activating 5′ hook functioning *in cis*.

induces a distinct conformational arrangement of the PB2 cap-binding subunit associated with a suppression of cap-dependent endonuclease activity (35). The influenza vRNA segments are used as templates for mRNA synthesis and replication whereas the cRNA templates only function for replication. It would be of interest to determine the relative stimulation of initiation of the influenza polymerase in the presence of the activating 5′ vRNA and 5′ cRNA ligands.

Activating Ligand Is Dependent on a Replicative Initiation. The finding that G0 and C1 are critical for activation of the RdRP links the activating potential of an RNA with the product of RNA replication. The prime-and-realign model posits that the G0 and C1 residues are first made as a dinucleotide primer following internal initiation at the C2 position of the 3′ promoter (11, 12). In our experiments, single nucleotide substitutions to G0 and C1 of the 5′ RNA ablate activation of RdRP. The C1 substitution can be rescued, however, by substitutions that restore base pairing between C1 and G7 of the 5′ RNA. Elimination of G0 or its substitution blocked activation linking the activating ligand to a bona fide replication initiation event. We observed that position G2 was tolerant of substitution in the activating RNA. During an infection, position G2 is the first nucleotide incorporated following realignment of the dinucleotide primer during prime-and-realign replication. The G2 templating nucleotide—position C2 of the promoter—is required to permit initiation to generate the pppGpC dinucleotide primer and thus templates the G0 of the activating ligand. This would ensure that, although the activating ligand can tolerate an alternate nucleotide at position +2, such an RNA is not produced during a replicative initiation event.

Origins of the Activating 5′ RNA Ligand. There are two possible sources of the 5′ RNA: a 5′ RNA structure that functions *in cis* from the same viral RNP that is being used as template (Fig. 5*B*), or short noncoding RNA ligands similar to small viral RNAs (svRNAs) generated by the heterotrimeric RdRP of influenza virus (33, 34, 36). Evidence from the current study suggests that L is most efficiently activated when the 3′ and 5′ RNAs are present at a 1:1 ratio. Although this does not preclude short RNAs functioning as activators *in trans*, we interpret this as evidence in support of a *cis* preference for such activation. The ability of an RNA to activate is also dependent upon the presence of the pseudotemplated G residue that is the product of prime-and-realign initiation during replication. We posit that, during replication, the 5′ end of the nascent RNA engages in intramolecular base pairing that promotes binding of free L, thereby assembling a preactivated polymerase complex for engagement of the 3′ promoter once it has been synthesized by the elongating polymerase. The context-dependent activation of L in the presence of corresponding vRNA–vRNA and cRNA–cRNA template–ligand combinations implies some degree of selectivity for this mechanism of RNA synthesis—selectivity that would be diminished in the presence of abundant svRNAs of both categories at the sites of viral replication. Despite this, the existence of L-synthesized svRNAs during arenavirus infections is an open question.

In summary, our study provides evidence in support of a model whereby arenavirus L proteins associated with genomic or antigenomic RNA segments are activated through direct interaction with the 5′ viral RNA sequences, in coordination with their respective 3′ promoter regions. The functionality of these activating 5′ termini is entirely dependent upon the prime-and-realign mechanism of arenavirus genome replication. Highly conserved sequences in both the 3′ and 5′ termini mediate panhandle duplex separation and 5′ structure formation for activation of the arenavirus polymerase. This conservation among SNS virus polymerases for a structured 5′ RNA ligand to activate polymerase raises the tantalizing possibility of pursuing the ligand and its binding pocket as targets for therapeutic intervention. The high degree of conservation of terminal sequences among all *Mammarenavirus* members might facilitate development of molecules to hinder the replication of both Old World and New World arenaviruses. Support for this idea is strengthened by the recent demonstration that a similar 5′ vRNA can activate the L polymerase of Lassa fever virus (37).

Materials and Methods

Protein Expression and Purification. Full-length WT and catalytically inactive (SDD1328AAA) MACV L (GenBank accession no. AAT40450.1) were expressed in adherent *Spodoptera frugiperda* cells (*Sf*21) via recombinant baculovirus-mediated protein expression, as described previously (20, 38). The proteins

were subsequently purified via Ni-affinity and size-exclusion chromatography, using HisTrap HP and Superdex 200 columns (GE Healthcare), respectively (*SI Appendix*, Fig. S1).

Negative-Stain Electron Microscopy. Purified MACV L at 0.02 mg·mL^{-1} was applied to carbon-coated copper grids (Ted Pella) and stained with 0.75% (wt/vol) uranyl formate immediately before imaging. Transmission electron microscopy images were collected using a Tecnai T12 microscope with a lanthanum hexaboride filament at 67,000× magnification and a defocus of −1.5 μm, as described previously (20).

MACV L in Vitro RNA Synthesis. Reconstituted assays for MACV L RNA synthesis were performed as described previously (38), with some modifications. MACV L was incubated at a final concentration of 0.16 μM in transcription buffer (50 mM Tris·HCl, pH 7.0, 50 mM NaCl, 10 mM KCl, 5 mM $MgCl_2$, 1 mM DTT, and 0.1 mg·mL^{-1} BSA) supplemented with 1 mM ATP, UTP, and CTP, and 0.16 μM (~5 μCi) [α-^{32}P]-GTP (PerkinElmer) and 80 μM GpC dinucleotide primer (Dharmacon). Reactions included 10 μM chemically synthesized 3′ template and 5′ activator oligos (IDT) except where indicated. The sequences of the RNA oligos are shown in *SI Appendix*, Tables S1 and S2.

Reactions were initiated by preincubation of the vRNAs and GpC primer at 65 °C in double-distilled H_2O (ddH_2O) for 5 min, followed by cooling on ice for 3 min. Transcription buffer was added as a 5× concentrate, followed by addition of purified MACV L. The reactions were then sequentially supplied with 0.5 μL of [α-^{32}P]-GTP (10 μCi·μL^{-1}), followed by the addition of cold NTPs as a 10× concentrate, bringing the final reaction volumes to 10 μL. Reactions were incubated at 30 °C for 3 h, terminated with 2× STOP solution (95% vol/vol deionized formamide, 20 mM EDTA), and heated to 95 °C for 2 min. Following inactivation, 6 μL of each reaction was separated by electrophoresis into a 36-cm-long polyacrylamide-urea (7 M) sequencing gel, 70 W for 1.5 h in 0.5× tris-borate-ethylenediaminetetraacetic acid (TBE). Gels were exposed for 5 h using a phosphor screen (GE Healthcare), and the radiolabeled RNA products were visualized using a Typhoon FLA 9500 scanner (GE Healthcare). The relative abundances of full-length RNA products (19 to 21 nt) were quantified using ImageJ, accounting for the subtraction of background noise and normalization among samples within individual experiments. All quantifications are shown with the SD from the mean of independent experiments.

The 5′ Ligand Folding Predictions. The secondary structure predictions for the MACV 5′ RNAs were analyzed using the web-based mfold version 2.3 algorithm at unafold.rna.albany.edu, with default parameters for RNA, except for a folding temperature set to 30 °C (39). The ΔG values and the number of predicted folding structures for each 5′ ligand are provided in *SI Appendix*, Table S1.

ACKNOWLEDGMENTS. Members of the S.P.J.W. laboratory provided insightful discussions, advice, and encouragement. Joshua Horwitz and Melissa Chambers supported negative-stain EM imaging. Robin Ross and Erica Gardner supported MACV L expression and purification, and Louis-Marie Bloyet and Benjamin Morin provided advice on the reconstituted RNA synthesis assays. This project was supported by NIH Grants AI133689 (to J.D.P.), T32AI007245 (to S.P.J.W.), and AI059371 (to S.P.J.W.).

1. Meyer BJ, Southern PJ (1993) Concurrent sequence analysis of 5′ and 3′ RNA termini by intramolecular circularization reveals 5′ nontemplated bases and 3′ terminal heterogeneity for lymphocytic choriomeningitis virus mRNAs. *J Virol* 67:2621–2627.
2. Polyak SJ, Zheng S, Harnish DG (1995) 5′ termini of Pichinde arenavirus S RNAs and mRNAs contain nontemplated nucleotides. *J Virol* 69:3211–3215.
3. Raju R, et al. (1990) Nontemplated bases at the 5′ ends of Tacaribe virus mRNAs. *Virology* 174:53–59.
4. Lehmann M, et al. (2014) Role of the C terminus of Lassa virus L protein in viral mRNA synthesis. *J Virol* 88:8713–8717.
5. Lelke M, Brunotte L, Busch C, Günther S (2010) An N-terminal region of Lassa virus L protein plays a critical role in transcription but not replication of the virus genome. *J Virol* 84:1934–1944.
6. Morin B, et al. (2010) The N-terminal domain of the arenavirus L protein is an RNA endonuclease essential in mRNA transcription. *PLoS Pathog* 6:e1001038.
7. Reguera J, et al. (2016) Comparative structural and functional analysis of bunyavirus and arenavirus cap-snatching endonucleases. *PLoS Pathog* 12:e1005636.
8. Lee KJ, Perez M, Pinschewer DD, de la Torre JC (2002) Identification of the lymphocytic choriomeningitis virus (LCMV) proteins required to rescue LCMV RNA analogs into LCMV-like particles. *J Virol* 76:6393–6397.
9. López N, Jácamo R, Franze-Fernández MT (2001) Transcription and RNA replication of tacaribe virus genome and antigenome analogs require N and L proteins: Z protein is an inhibitor of these processes. *J Virol* 75:12241–12251.
10. Pinschewer DD, Perez M, de la Torre JC (2003) Role of the virus nucleoprotein in the regulation of lymphocytic choriomeningitis virus transcription and RNA replication. *J Virol* 77:3882–3887.
11. Garcin D, Kolakofsky D (1990) A novel mechanism for the initiation of Tacaribe arenavirus genome replication. *J Virol* 64:6196–6203.
12. Garcin D, Kolakofsky D (1992) Tacaribe arenavirus RNA synthesis in vitro is primer dependent and suggests an unusual model for the initiation of genome replication. *J Virol* 66:1370–1376.
13. Marq J-B, Kolakofsky D, Garcin D (2010) Unpaired 5′ ppp-nucleotides, as found in arenavirus double-stranded RNA panhandles, are not recognized by RIG-I. *J Biol Chem* 285:18208–18216.
14. Meyer BJ, Southern PJ (1994) Sequence heterogeneity in the termini of lymphocytic choriomeningitis virus genomic and antigenomic RNAs. *J Virol* 68:7659–7664.
15. Pflug A, Guilligay D, Reich S, Cusack S (2014) Structure of influenza A polymerase bound to the viral RNA promoter. *Nature* 516:355–360.
16. Reich S, et al. (2014) Structural insight into cap-snatching and RNA synthesis by influenza polymerase. *Nature* 516:361–366.
17. Hengrung N, et al. (2015) Crystal structure of the RNA-dependent RNA polymerase from influenza C virus. *Nature* 527:114–117.
18. Chang S, et al. (2015) Cryo-EM structure of influenza virus RNA polymerase complex at 4.3 Å resolution. *Mol Cell* 57:925–935.
19. Gerlach P, Malet H, Cusack S, Reguera J (2015) Structural insights into Bunyavirus replication and its regulation by the vRNA promoter. *Cell* 161:1267–1279.
20. Kranzusch PJ, et al. (2010) Assembly of a functional Machupo virus polymerase complex. *Proc Natl Acad Sci USA* 107:20069–20074.
21. Fodor E, Pritlove DC, Brownlee GG (1994) The influenza virus panhandle is involved in the initiation of transcription. *J Virol* 68:4092–4096.
22. Fodor E, Pritlove DC, Brownlee GG (1995) Characterization of the RNA-fork model of virion RNA in the initiation of transcription in influenza A virus. *J Virol* 69:4012–4019.
23. Fodor E, Palese P, Brownlee GG, García-Sastre A (1998) Attenuation of influenza A virus mRNA levels by promoter mutations. *J Virol* 72:6283–6290.
24. Pritlove DC, Fodor E, Seong BL, Brownlee GG (1995) In vitro transcription and polymerase binding studies of the termini of influenza A virus cRNA: Evidence for a cRNA panhandle. *J Gen Virol* 76:2205–2213.
25. Pritlove DC, Poon LLM, Devenish LJ, Leahy MB, Brownlee GG (1999) A hairpin loop at the 5′ end of influenza A virus virion RNA is required for synthesis of poly(A)+ mRNA in vitro. *J Virol* 73:2109–2114.
26. Pritlove DC, Poon LLM, Fodor E, Sharps J, Brownlee GG (1998) Polyadenylation of influenza virus mRNA transcribed in vitro from model virion RNA templates: Requirement for 5′ conserved sequences. *J Virol* 72:1280–1286.
27. Tiley LS, Hagen M, Matthews JT, Krystal M (1994) Sequence-specific binding of the influenza virus RNA polymerase to sequences located at the 5′ ends of the viral RNAs. *J Virol* 68:5108–5116.
28. Poon LLM, Pritlove DC, Sharps J, Brownlee GG (1998) The RNA polymerase of influenza virus, bound to the 5′ end of virion RNA, acts in cis to polyadenylate mRNA. *J Virol* 72:8214–8219.
29. Ferron F, Weber F, de la Torre JC, Reguera J (2017) Transcription and replication mechanisms of *Bunyaviridae* and *Arenaviridae* L proteins. *Virus Res* 234:118–134.
30. Hass M, et al. (2006) Mutational analysis of the lassa virus promoter. *J Virol* 80:12414–12419.
31. Perez M, de la Torre JC (2003) Characterization of the genomic promoter of the prototypic arenavirus lymphocytic choriomeningitis virus. *J Virol* 77:1184–1194.
32. Patterson M, et al. (2014) Rescue of a recombinant Machupo virus from cloned cDNAs and in vivo characterization in interferon (αβ/γ) receptor double knockout mice. *J Virol* 88:1914–1923.
33. Perez JT, et al. (2010) Influenza A virus-generated small RNAs regulate the switch from transcription to replication. *Proc Natl Acad Sci USA* 107:11525–11530.
34. Perez JT, et al. (2012) A small-RNA enhancer of viral polymerase activity. *J Virol* 86:13475–13485.
35. Thierry E, et al. (2016) Influenza polymerase can adopt an alternative configuration involving a radical repacking of PB2 domains. *Mol Cell* 61:125–137.
36. Umbach JL, Yen H-L, Poon LLM, Cullen BR (2010) Influenza A virus expresses high levels of an unusual class of small viral leader RNAs in infected cells. *MBio* 1:e00204-10.
37. Vogel D, Rosenthal M, Gogrefe N, Reindl S, Günther S (March 29, 2019) Biochemical characterization of the Lassa virus L protein. *J Biol Chem*, 10.1074/jbc.RA118.006973.
38. Kranzusch PJ, Whelan SPJ (2011) Arenavirus Z protein controls viral RNA synthesis by locking a polymerase-promoter complex. *Proc Natl Acad Sci USA* 108:19743–19748.
39. Zuker M (2003) Mfold web server for nucleic acid folding and hybridization prediction. *Nucleic Acids Res* 31:3406–3415.